

Determination of the textural characteristics of carbon samples using scanning electronic microscopy images: comparison with mercury porosimetry data

A. C. Alvarez · N. Passé-Coutrin · S. Gaspard

Received: 1 November 2012 / Accepted: 23 February 2013 / Published online: 13 March 2013
© Springer Science+Business Media New York 2013

Abstract In this paper, scanning electron microscopy (SEM) images of carbon samples were analysed, and some textural characteristics were obtained and compared with those determined using mercury porosimetry data. Fractal dimensions were calculated from both mercury porosimetry and SEM images as methods for characterising the porous distribution (heterogeneity) of the samples. Lacunarity is easily determined from SEM images as a measure of the degree of heterogeneity of a porous surface. A relationship between the lacunarity and the fractal dimensions calculated using both methods is shown. Pore-size distributions were also determined from the analysis of SEM images. We show that the analysis of SEM images is a valuable complement to mercury porosimetry measurements and a useful tool for the characterisation of porous surfaces. This method offers the possibility of evaluating the features of porous materials and comparing the results to those obtained using mercury intrusion analysis.

Keywords Fractal dimension · Lacunarity · Activated carbons · Scanning electronic microscopy · Pore size · Mercury porosimetry

1 Introduction

Fractal dimension theory (Mandelbrot 1975) is a useful tool for the characterisation of the structure of porous materials. This theory is based on the concept of self-similarity. An object is self-similar if its appearance does not depend on the scale at which it is observed. Intrusion mercury volume data can be processed in the context of fractal theory (Mahamud et al. 2003), thereby allowing a recently used parameter, the fractal dimension (Gaspard et al. 2006), to be determined. In this paper, the fractal dimensions of ten activated carbon samples was calculated from mercury porosimetry data based on the method presented by Mahamud and Novo (2008). To estimate the fractal dimension from mercury porosimetry data, the linear increase in the mercury cumulated volume due to compression rather than intrusion when pressure is applied to a material was considered (Passé-Coutrin et al. 2005).

The weakness of such indirect methods is that they are based on mathematical models that do not always match with observed behaviour of activated carbons. For example, mercury porosimetry theory assumes an idealised cylindrical pore model as the basis for estimating the average pore width of activated carbons. However, scanning electron microscopy (SEM) micrograph observations have shown that this model does not always reflect the complex nature of porosity in activated carbons. Furthermore, the fractal dimension generally exhibit different values depending on the method used (Tatlyer and Erdem-Suenatalar 1999; Gauden et al. 2001).

Scanning electron microscopy is a direct method that is useful for the characterisation of the textural structure of pores (Ball and McCartney 2011; Achaw and Afrane 2008). The standard SEM image represents a two-dimensional (2D) structure from which mostly qualitative data

A. C. Alvarez
Oceanology Institute, Environmental Agency, Avenida Primera,
18406, Flores, Playa, 11600 C. Habana, Cuba
e-mail: meissa98@impa.br

N. Passé-Coutrin · S. Gaspard (✉)
Laboratoire COVACHIM-M2E EA 3592, Université des
Antilles et de la Guyane, P.O. Box 250, 97157 Pointe-à-Pitre
Cedex, France
e-mail: sgaspard@univ-ag.fr

N. Passé-Coutrin
e-mail: npasseco@univ-ag.fr

can be extracted. 2D SEM cannot be used to observe the three-dimensional (3D) porosity of the materials because conventional SEM instruments cannot observe the inner parts of a material. Therefore, a precise description that represents the 3D pore structure is difficult. Nevertheless, this method is easy to apply, and data obtained from the observed images can be improved through the use of appropriate image-processing methods. Fractal dimensions are sometimes insufficient to characterise the heterogeneity of samples because different textures can exhibit similar fractal dimensions. Such estimations can be improved through the use of the lacunarity (Kilic and Abiyev 2011), which can be obtained from SEM images and which gives a measurement of the heterogeneity of holes between pores in the surface of activated carbon.

Given the previously described advantages and drawback of SEM and mercury porosimetry, we propose to use these direct and indirect methods, respectively, as alternative methods for obtaining information about the textural characteristics of porous materials. This study is focused on combining fractal dimension and lacunarity data obtained from 2D SEM images to provide new insight into the texture of porous materials and to allow a comparison of the results with those from mercury porosimetry data.

The pore-size distribution (PSD) function is usually used as a quantitative characteristic of the porous structure of solid adsorbents with respect to their heterogeneity. The PSD function of a porous medium is perhaps the most important characteristic because it influences the transport of sorbates in the structure. In this study, we compare the PSDs obtained from mercury porosimetry and SEM images. This analysis will contribute not only to the search for alternative methods to characterise the distribution of the pores but also to search for information that can reduce the uncertainties related to the texture characterisation of the material.

In the method presented here, fractal dimensions, PSDs and lacunarities from SEM images were determined on the same set of experimental data. Fractal dimension values obtained either from SEM analysis or from mercury porosimetry are compared. The relationship between the lacunarity and the fractal dimension are discussed. In addition, we discuss the differences between the two concepts.

2 Materials and methods

2.1 Preparation of carbon samples

The samples studied here were prepared from different precursors: *Posidonia oceanica* (a marine biomass), sugar cane bagasse and vetiver roots. Preparation chars from raw

P. oceanica fibres were prepared by the carbonisation of the fibres at 300 and 400 °C, which resulted in samples PosPyr300 and PosPyr400, respectively. *Posidonia oceanica* fibres were also pyrolysed at 600 °C during 1 h, the carbon sample obtained was further activated by steam for 20, 120 and 300 min giving samples PAC20, PAC120 and PAC300, respectively (Ncibi et al. 2009). Activated carbon samples obtained by chemical activation were prepared by phosphoric acid impregnation of either bagasse or vetiver roots in H₃PO₄ (85 %) for 24 h followed by pyrolysis at 600 °C. Impregnation ratios, X_P (g H₃PO₄/g precursor), of 0.5:1; 1:1 and 1.5:1 were used to produce samples VetP0.5, VetP1, VetP1.5, BagP0.5 and BagP1, respectively (Altenor et al. 2009). The complete procedures for the preparations of carbons and the corresponding textural characteristics are described in detail elsewhere (Passé-Coutrin et al. 2008; Altenor et al. 2009; Ncibi et al. 2009).

2.2 Scanning electron microscopy

A SEM equipped with an energy-dispersive X-ray micro-analyser (Hitachi S-2500) was used to determine the surface textural characteristics. The char samples were first mounted on an aluminium stub. The microscope was operated at an accelerating voltage of 200 kV and at a working distance of 35 mm. Utilising the ImageJ software (<http://rsbweb.nih.gov/ij/>), we obtained quantitative information from 2D SEM images of activated carbon samples. However, this process involves a number of challenges. These include the sample preparation, the scanning process, the image formation and the image analysis. The quantitative data are the pore-structure, the pore sizes, the pore shapes, the pore surface area and the PSD, which are most useful data for characterisation. Because of the complexity of the system studied, a complete analysis must be performed together with the qualitative analysis.

2.3 Determination of fractal dimensions, lacunarities and pore-size distributions from SEM images

The analysis of SEM images was performed using the ImageJ software developed for direct qualitative and quantitative images analysis. ImageJ is a public domain, Java-based image processing program developed at the National Institutes of Health.

This software allows preprocessing of the image via several filters and, scale adjustments, to enable the selection of the best part of the image; and finally, a binarisation is performed. Fractal dimension D_{SEM} was determined by using the box-counting method. Lacunarity was calculated by the sliding box method. This procedure was applied to the images in Figs. 1 and 2, which were processed in a manner similar to that reported by Gun'ko et al. (2012).

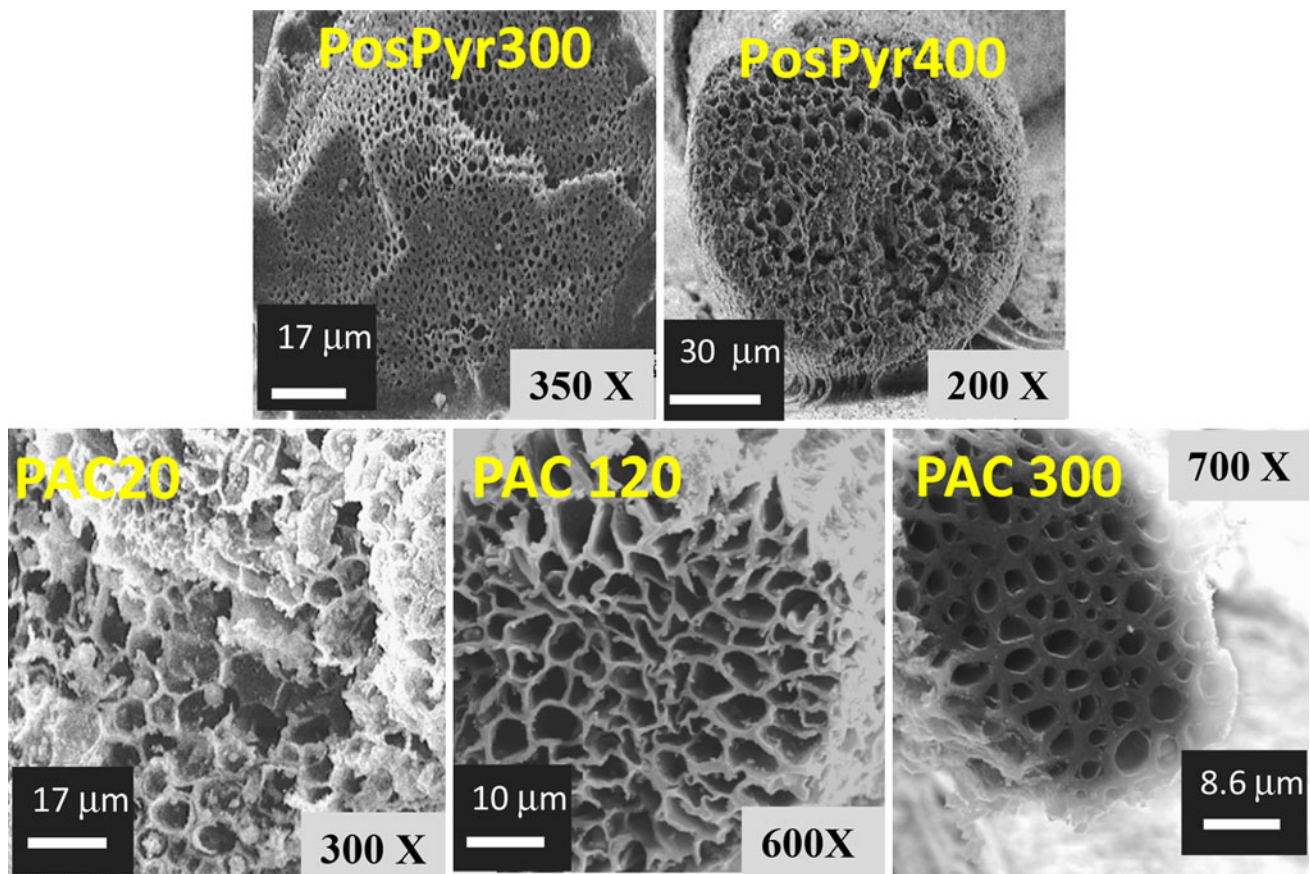


Fig. 1 SEM micrographs of carbon samples prepared from *Posidonia oceanica*. Each micrograph represents a fragment of the porous surface

Lacunarity measures heterogeneity. This quantity was designed to complement fractal analysis when fractal dimension values are similar (Mandelbrot 1975, 1983), i.e., to show qualitative differences in the mass distribution, or differences in the amount of holes. The determination of the lacunarity is based on pixel masses instead of box counts. The word “lacunarity” literally refers to a *gap* or *pool*, as derived from the word for “lake”; however, in morphological analysis, it has been variously defined as gappiness, visual texture, inhomogeneity, translational and rotational invariance, etc. Allain and Cloitre (1991) defined quantitatively lacunarity as the mean-square deviation of the fluctuations of the mass distribution function divided by its square mean. They also defined it as the width of the mass distribution function for the set of points, given the “boxsize”. Therefore, greater values of lacunarity imply greater heterogeneity because it indicates a wider mass distribution function for the set points, which, in turn, means a greater number of different mass values. Usually denoted as Λ or λ , the lacunarity pertains to both the gaps and the heterogeneity observed in the ImageJ software. The determination of lacunarity values based on box counting via the gliding-box method is performed using the pixel distribution (Przemyslaw 2009). To find the pixel

distribution, the number of pixels in each ε -sized box in a grid placed on an image is counted during standard non-overlapping or overlapping box counting. Then, the lacunarity, or λ , for each grid of calibre ε is calculated from the standard deviation, σ , and mean, μ , for pixels per box. A λ value exists for each ε in each series of grid sizes in each grid orientation, g , in a set of grid orientations.

ImageJ is designed with an open architecture that provides extensibility via Java plugins and recordable macros. Custom acquisition, analysis and processing plugins can be developed using ImageJ’s built-in editor and a Java compiler. User-written plugins make possible to solve many image processing and analysis problems, from 3D live-cell imaging. To produce the PSD from SEM images we followed the steps: scaling the images knowing the distance in micrometer and equivalence in pixel on the image followed by the command (*Analyze>Set Scale*), after we preprocess the image with an appropriate filter, for example (command *Image>Adjust>>*) or (command *Process>filters*), converting the image to grayscale 8 bit and binarisation (command *Process>binary>make binary*). Further, the particles size analysis (command *Analyze>>Analyze particle*) and (command *Analyze>>Distribution*) which produces a complete characterization of pore size and amount of pores. Finally

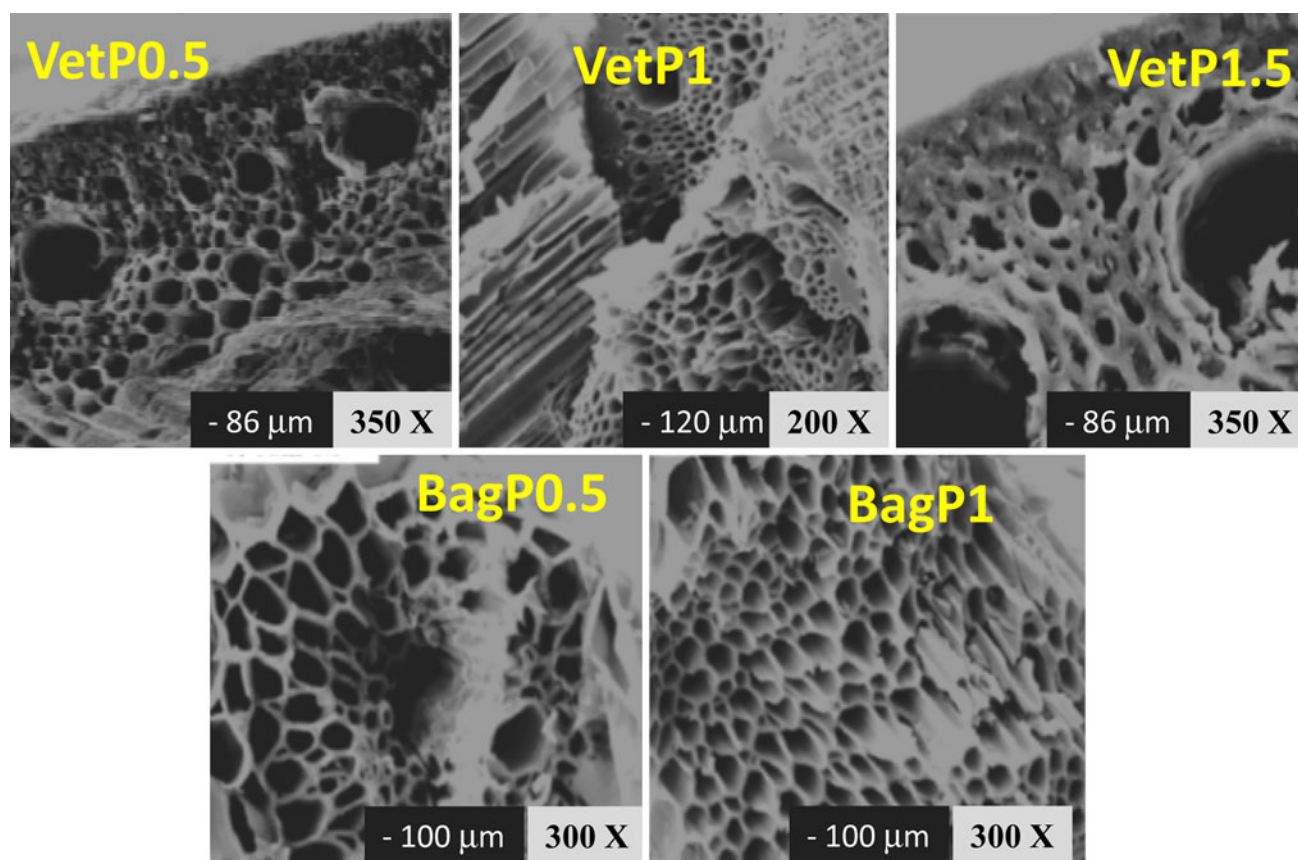


Fig. 2 SEM micrographs of carbon samples prepared from *Posidonia oceanica*. Each micrograph represents a fragment of the porous surface

we use the distribution options in the analysis panel that produces the porous-size distribution according to different parameter, assuming a circular form of the pores.

Determination of fractal dimension and lacunarity requires the installation on ImageJ of the pluggins *Fractal Analysis* (<http://rsb.info.nih.gov/ij/plugins/index.html>). Once we open the binary image, to produce the fractal dimension D and lacunarity, we select the command *Plugins>Fractal Analysis*. On above mentioned pluggins, we take the *Standard Box Count* option to estimate the fractal dimension and *Sliding box lacunarity* option for Lacunarity.

2.4 Mercury porosimetry data

Mercury porosimetry of the samples was performed using a Thermo Finnigan porosimeter, which provides a maximum operating pressure of 200 MPa. The data obtained consisted of records of the volume of mercury intruded as a function of pressure. This technique is based on the fact that mercury does not wet most substances and will therefore not penetrate pores by capillary action unless it is forced to do so. Liquid mercury has a high surface tension and also exhibits a high contact angle against most solids. Its entry into pore spaces requires the application of pressure in inverse proportion to the pore diameter.

2.5 Fractal dimension from mercury porosimetry data

Estimation of the fractal dimension from the mercury porosimetry data was performed according to the methods reported in the literature (Friesen and Mikula 1987; Passé-Coutrin et al. 2005). The following relationship was used:

$$\frac{dV}{dP} = P^{4-D_{\text{poro}}},$$

where V is the volume that penetrates the porous medium at pressure P , and D_{poro} is the fractal dimension. This equation allows a value to be obtained for the fractal dimension, D_{poro} , from the plot $\ln(dV/dP)$ versus $\ln P$. Because coals are compressible materials, the experimental data from mercury porosimetry must be corrected prior to their analysis. To do so, we used the method described by Mahamud et al. (2003).

3 Results and discussion

Scanning electron microscopy micrographs of small fragments of carbon samples chosen arbitrarily are presented in Figs. 1 and 2. A cursory examination reveals that the external porous surfaces of the different carbon fragments

Table 1 Fractal dimension, lacunarity and minimum and maximum porous size of SEM micrograph from ImageJ software calculations

| Carbon sample | Fractal dimension D_{SEM} | Lacunarity | Minimum diameter (μm) | Maximum diameter (μm) |
|---------------|-----------------------------|------------|------------------------------------|------------------------------------|
| PosPyr300 | 1.8691 | 0.1758 | 3.56 | 110.6 |
| PosPyr400 | 1.8481 | 0.1528 | 1.14 | 20.73 |
| PAC20 | 1.8549 | 0.1834 | 0.33 | 21.87 |
| PAC120 | 1.8116 | 0.2592 | 0.28 | 10.64 |
| PAC300 | 1.8371 | 0.1605 | 0.24 | 4.86 |
| VetP0.5 | 1.8253 | 0.2332 | 3.94 | 137.4 |
| VetP1 | 1.8395 | 0.188 | 0.24 | 6.91 |
| VetP1.5 | 1.8076 | 0.2827 | 16.17 | 232 |
| BagP05 | 1.8205 | 0.2062 | 18.81 | 359 |
| BagP1 | 1.8395 | 0.188 | 18.81 | 353.3 |

exhibit a high porosity but different textures. Pores of some samples were difficult to distinguish due to different brightness and shadows. These results imply that an appropriate image preprocessing step is necessary in these cases. The images were cropped to enable the characterisation of a more probable texture of the samples.

For chars derived from *P. Oceanica* (Ncibi et al. 2009), which were produced under several pyrolysis temperatures, as the pyrolysis temperature was increased from 300 to 400 °C, the fibrous chars showed more pores in their inner structures (Fig. 1). Activated carbon samples PAC120 and PAC20 were slightly obstructed by carbonaceous materials that were deposited during the cooling period after the pyrolysis procedure (Ncibi et al. 2009). In this case, a carefully preprocessing was performed, the pores were well distinguished in the binarised images.

Figure 2 shows that all the samples exhibit a clearly developed porous network. In addition, sample VetP1 exhibits macropores and a stripy texture, which made the surface texture analysis difficult. Some differences in textures are evident. For example, a comparison of the BagP0.5, BagP1, VetP05, and VetP1.5 surfaces reveals that the latter has a more heterogeneous pattern. The SEM images also show that the pores of BagP0.5 are well defined compared to those of Vetp1.5. Samples VetP0.5, BagP1 and BagP0.5 exhibit similar pore size, while samples VetP1, VetP0.5, PAC120 and PAC20 exhibit wider pores.

Table 1 gives the data obtained from SEM images analysis using the ImageJ software, including the fractal dimensions, the lacunarities, and the minimum and maximum pore diameters of the porous samples shown in Figs. 1 and 2. The fractal dimension of the sample shown in the micrograph in Fig. 1 is between 1 and 2 (Table 1), which corresponds with the fact that estimates of the 2D structure of the surface outside of the pores is considered. Notably, all of the samples exhibit similar fractal dimensions of ~ 1.8 , despite the samples having different

appearances. The structural differences can be discriminated through the lacunarity. Although low lacunarity values were obtained in all cases, they were slightly different. Samples with lower lacunarity, such as for PosPyr400, showed less diversity in pore size (Fig. 1). However, sample VetP1 showed the greatest lacunarity value, with a spatial distribution that corresponds to a more heterogeneous texture. Thus, a simple inspection shows that lacunarity is a valuable parameter in describing small differences in the spatial distributions of pores.

The lacunarity values were low, which was expected because all of the samples exhibit high porosity with low spatial heterogeneity. However, despite the small differences between the lacunarity values, this parameter reflects the distinct texture of the samples. The lacunarity value determined from the SEM micrograph of PosPyr300 is 0.1758, and the texture of the sample differs from that of VetP0.5, whose SEM micrograph indicates a lacunarity of 0.2332, which indicates a more heterogeneous spatial distribution of holes.

The minimum and maximum pore diameters are given in Table 1. These parameters are essential for completing the characterisation of texture because they show the range of possible diameters of the pores, which can be different even if the fractal dimension and lacunarity are similar. Activated carbon samples VetP1, PAC120, PAC20, and PAC200 exhibited the lowest values of minimum diameter, whereas samples BagP05 and BagP1 exhibited the greatest values.

The highest fractal dimensions observed using mercury porosimetry D_{poro} (between 2.5 and 2.8) were obtained for the activated carbons prepared via the phosphoric acid activation of bagasse and vetiver roots. However, carbons obtained via the pyrolysis of *P. Oceanica* exhibited lower fractal dimensions. The calculation of the fractal dimension from mercury porosimetry assumes cylindrical pores (Mahamud et al. 2003). A fractal dimension of approximately 3 indicates that the porous system contains many convolutions

(i.e., twists and turns) that occupy nearly the whole volume, as is the case of the samples prepared via chemical activation of bagasse and vetiver roots. A large compressibility may be linked to thin pore walls. This result appears to be in agreement with the large fractal dimension when the porous system is settled in the whole volume (i.e., samples VetP1, VetP1.5, BagP1, and BagP0.5).

Figures 3 and 4 show the PSDs obtained from mercury porosimetry experiments and SEM analyses, respectively. In the case of mercury porosimetry, the y-axis represents the percent of intrusion volume for each interval size, whereas, for SEM analyses, it represents the number of pores of each pore size (Fig. 4). Based on the pore distribution (Fig. 3), the two activated carbon samples VetP1 and VetP0.5 have porous textures that are different from those of the BagP0.5 and BagP1 activated carbon samples.

The first correlation noted is that between the lacunarity and the fractal dimensions obtained through SEM analysis. An initial correlation analysis of the 10 samples shown in Fig. 5a indicated an acceptable linear relationship with $R = 0.81$. The exclusion of the data points that correspond to the typical samples PosPyr30, PAC300 and BagP0.5 resulted in a greater correlation, with $R = 0.92$ (Fig. 5b). This improved correlation could be explained by the fact that the typical samples PosPyr300 and PAC300 exhibit lower lacunarity values (i.e., 0.1758 and 0.1605, respectively) but also exhibit fractal dimensions similar to that of sample BagP0.5, which has a higher lacunarity (0.2062).

Lacunarity analysis using the previously discussed values (Table 1) showed that data sets extracted from complex fractals exhibited little pattern change, i.e., they exhibited similar fractal dimensions. In addition, homogeneous textures exhibit low lacunarity. However, when spatial heterogeneity features increase slightly, lacunarity values also tend to increase. In some instances, fractal dimensions and lacunarity values are correlated, in agreement with previously published work (Armatas et al. 2002; Przemyslaw 2009).

When the fractal dimensions from mercury analysis were correlated with the lacunarity from SEM data, no significant correlation was observed when all of the samples were considered. However, for some subsets of data, a correlation was found (see Fig. 5e, f). This correlation may be related to the facts that lacunarity is representative of a transept of the porous medium and that the surface behaviour is maintained on the inside of the porous medium only in some cases.

Another issue is that such quantities measured in the external portion of a porous material are expected to bear some relationship with those measured in the interior of the material. The micrograph images (Figs. 1, 2) clearly represent part of the outer surface of the porous media; therefore, the minimum and average pore sizes have a

direct influence on transport of molecules inside the solid. This minimum pore size interval was detected using both the mercury porosimetry method and the method of SEM image analysis. Therefore, the minimum pore size can be calculated for all of the samples.

In the cases of the PosPyr300 (Fig. 1), VetP1.5, BagP0.5, BagP1 and VetP0.5 activated carbon samples (Fig. 2), the range of the outer surface pore size determined using SEM analysis matches with the almost total interval described by the mercury porosimetry PSD (Figs. 3, 4). However, these coincidences do not indicate that the pore sizes determined from the SEM images represent the entire interval of pore sizes found in the interior of the porous material.

The fractal dimensions obtained using mercury porosimetry (Table 2) between 2 and 3 correspond to a 3D dimension because mercury is introduced inside the porous material and is capable of filling the 3D complex structure. In this case, the fractal dimensions for each carbon sample are significantly different. However, in view of the complex surface patterns that can be reproduced inside the porous materials, some degree of correlation between the D_{SEM} , the D_{poro} and the lacunarity is expected to be observed. The set of carbon samples studied showed an acceptable correlation for fractal dimension and lacunarity (see Fig. 5). This result may indicate that, in such cases, the surface texture is similar to the internal structure. On the other hand, in some cases, SEM analysis showed that the pores were not reached by the mercury in the mercury porosimetry method. In the cases of PAC300, VetP1, PAC120, PAC20, and PosPyr300, the pore sizes indicated by analyses of SEM images were lower than those obtained by mercury porosimetry.

In both cases, the information provided by SEM is clearly insufficient by itself to characterise the sample texture. However, complementary information about the pore structure can be obtained. Lacunarity, for example, is a value that cannot be obtained from mercury porosimetry. The fractal dimensions obtained from SEM images characterise only the outer pore surface, whereas the mercury porosimetry fractal dimensions describe the tridimensional internal features. However, the exterior surface characteristics are expected to be imitated inside the pores, although these characteristics cannot be completely represented by a 2D image of the pores. The acceptable correlation between the fractal dimensions obtained from mercury porosimetry and those obtained from SEM analysis (Fig. 5) may indicate that the internal pore structure is a continuation of what is displayed on the surface. The textural analysis performed via the processing of SEM data could consequently be used to guide various stages in the activation process of active carbons.

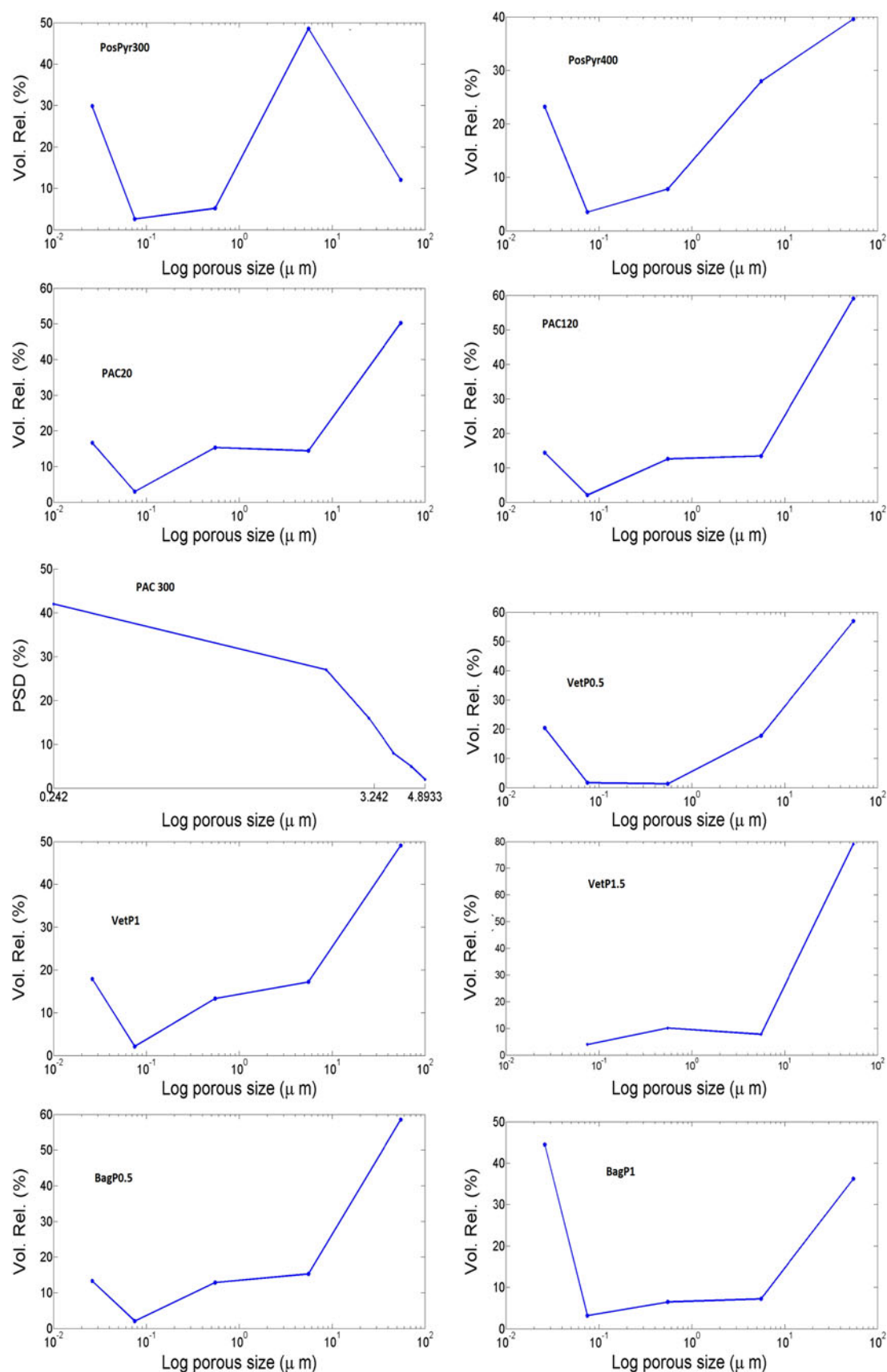


Fig. 3 Pore-size distributions of carbon samples based on mercury porosimetry measurements

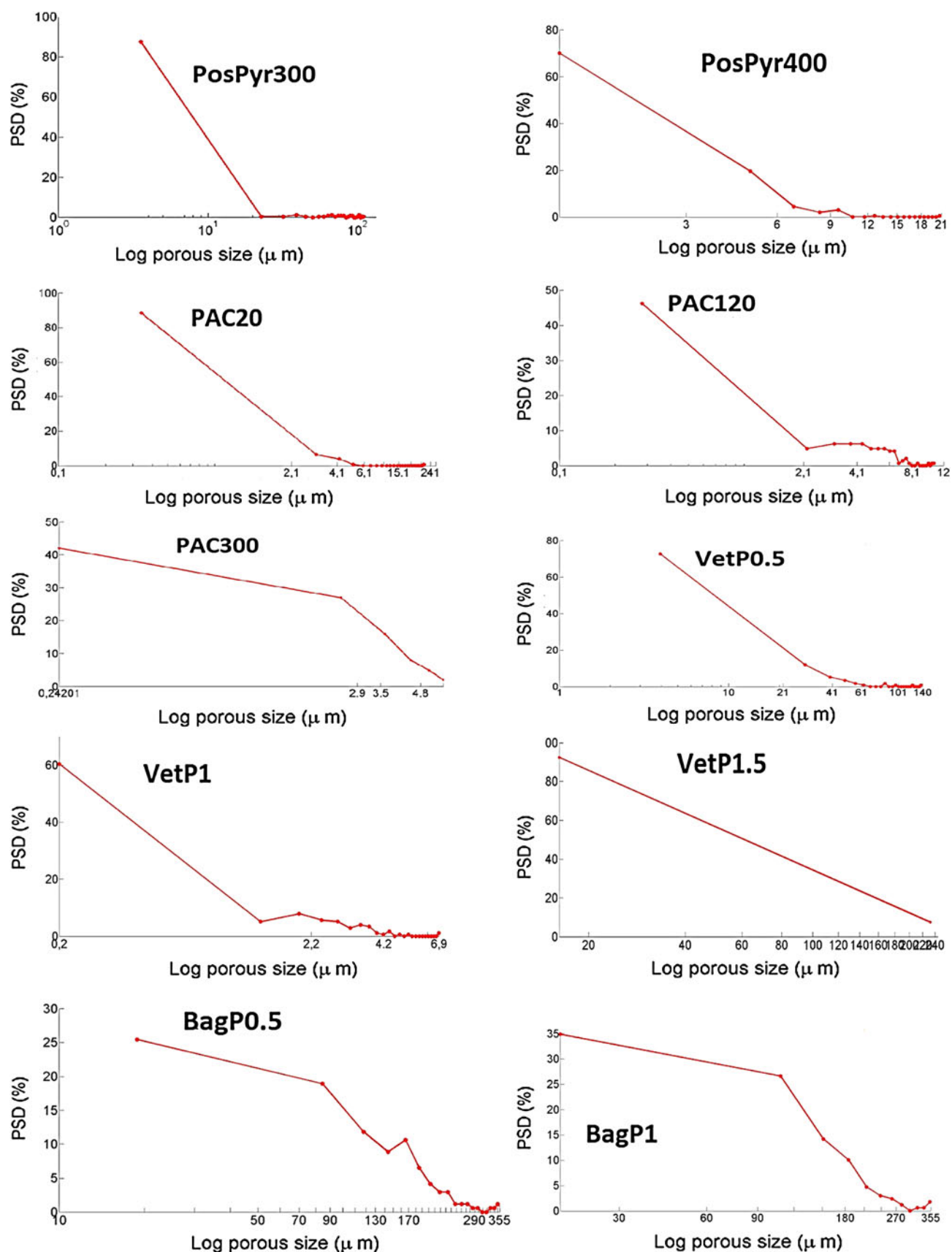


Fig. 4 Pore-size distributions of carbon samples based on SEM images analysis

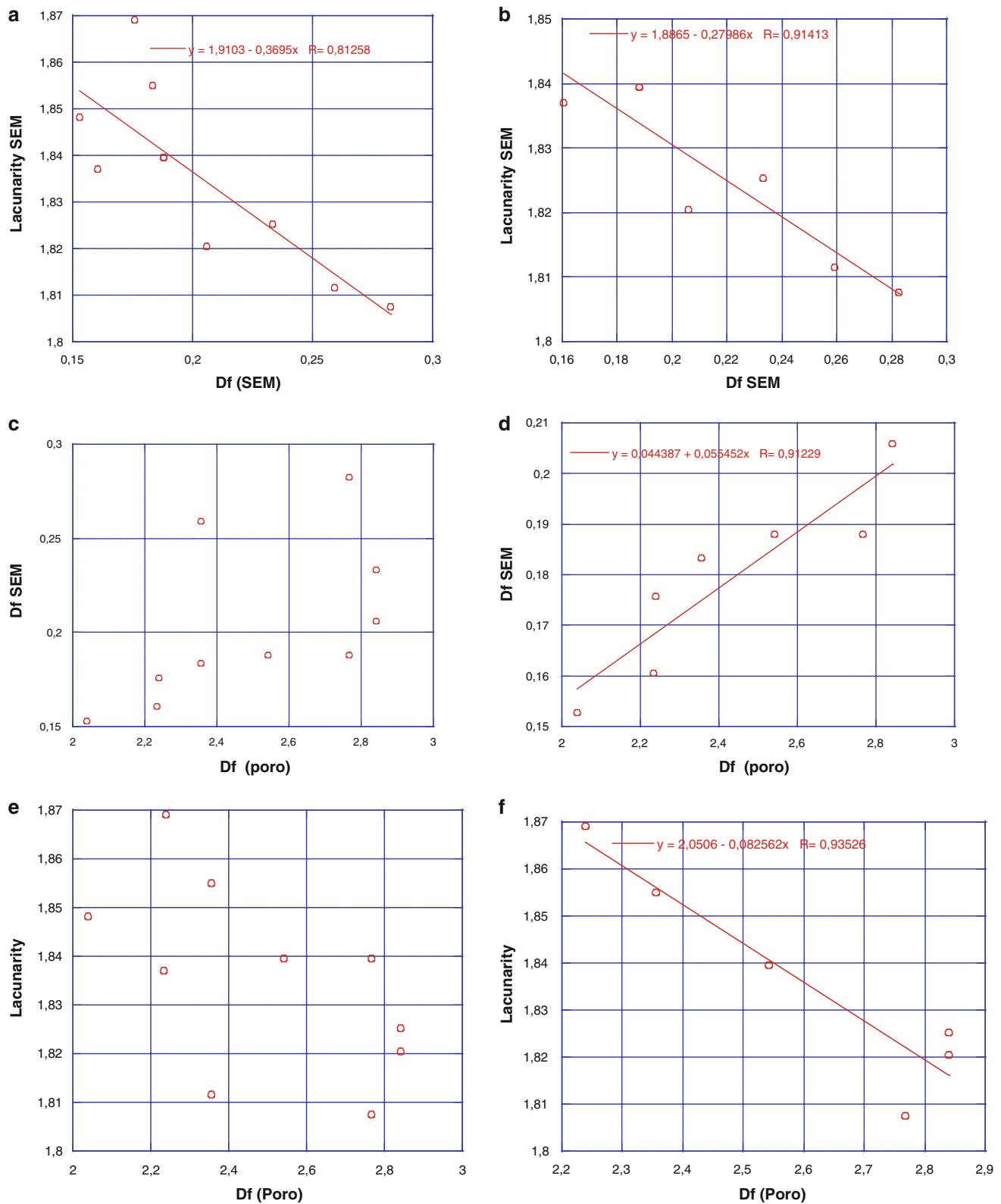


Fig. 5 Correlations between fractal dimensions and lacunarity obtained using SEM images analysis and fractal dimensions from mercury porosimetry: **a** lacunarity against Df_{SEM} for all samples; **b** lacunarity against Df_{SEM} for selected samples; **c** Df_{SEM} against

Df_{poro} for all samples; **d** Df_{SEM} against Df_{poro} for selected samples; **e** lacunarity against Df_{poro} for all samples; **f** lacunarity against Df_{poro} for selected samples

Table 2 Parameters calculated from mercury porosimetry: compressibility and fractal dimension of the porous surface

| Carbon sample | Compressibility 10–12 m ³ kg ⁻¹ Pa ⁻¹ | Fractal dimension D_{poro} |
|---------------|---------------------------------------------------------------------------|----------------------------------------|
| PosPyr300 | 1.45 | 2.2398 |
| PosPyr400 | 1.5037 | 2.0398 |
| PAC20 | 1.4615 | 2.3555 |
| PAC120 | 1.3626 | 2.3557 |
| PAC300 | 1.3551 | 2.2346 |
| VetP0.5 | 1.4024 | 2.7389 |
| VetP1 | 2.828 | 2.5416 |
| VetP1.5 | 2.8034 | 2.7680 |
| BagP0.5 | 2.0755 | 2.8407 |
| BagP1 | 3.5716 | 2.7251 |

4 Conclusions

The need to use both direct and indirect methods for texture analysis was demonstrated in this paper. The differences observed between the PSDs determined using SEM and that determined using mercury porosimetry were expected because mercury can reach the deep pores inside the carbon samples, whereas SEM provides only an image of the surface features. However, a coincidence occurs in at least some pores, as shown by the relationship between the fractal dimensions and the lacunarities obtained from the analysis of SEM images using the ImageJ software. The correlation between the fractal dimensions obtained from mercury porosimetry and those obtained from SEM analysis indicates that the internal pore structure is a continuation of what is displayed on the surface.

Acknowledgments I am grateful to the Frech Embassy in Cuba, Alex Meril and Ulises Jauregui for promoting scientific collaboration that has resulted in the development of works such as this report. We also thank the referees for their suggestions and remarks that allowed to improve our manuscript.

References

- Achaw, O.W., Afrane, G.: The evolution of pore structure of coconut shells during the preparation of coconut shell-based activated carbons. *Microporous Mesoporous Mater.* **112**, 284–290 (2008)
- Allain, C., Cloitre, M.: Characterizing the lacunarity of random and deterministic fractal sets. *Phys. Rev. A* **44**(6), 3552–3558 (1991)

- Altenor, S., Carene, B., Emmanuel, E., Lambert, J., Ehrhardt, J.J., Gaspard, S.: Adsorption studies of methylene blue and phenol onto vetiver roots activated carbon prepared by chemical activation. *J. Hazard. Mater.* **165**, 1029–1039 (2009)
- Armata, C.S., Kolonia, K.M., Pomoni, P.J.: Morphometry of porous solids: lacunarity, fractal dimensions, connectivity and some topological similarities with neurons. *Langmuir* **18**, 10421–10429 (2002)
- Ball, M.D., McCartney, D.G.: The measurement of atomic number and composition in a SEM using backscattered detectors. *J. Microsc.* **124**, 57–68 (2011)
- Friesen, W.I., Mikula, R.J.: Fractal dimensions of coal particles. *J. Colloid Interface Sci.* **120**(1), 263–271 (1987)
- Gaspard, S., Altenor, S., Passe-Coutrin, N., Ouensanga, A., Brouers, F.: Parameters from a new kinetic equation to evaluate activated carbons efficiency for water treatment. *Water Res.* **40**, 3467–3477 (2006)
- Gauden, P.A., Terzyk, A.P., Rychlicki, G.: The new correlation between microporosity of strictly microporous activated carbons and fractal dimension on the basis of the Polanyi–Dubinin theory of adsorption. *Carbon* **39**, 267–278 (2001)
- Gun'ko, V.M., Kozynchenko, O.P., Tennison, S.R., Leboda, R., Skubiszewska-Zieba, J., Mikhalovsky, S.V.: Comparative study of nanopores in activated carbons by HRTEM and adsorption methods. *Carbon* **50**(9), 3146–3153 (2012)
- ImageJ software. <http://rsbweb.nih.gov/ij>
- Kilic, K.I., Abiyev, R.H.: Exploiting the synergy between fractal dimension and lacunarity for improved texture recognition. *Signal Process.* **91**, 2332–2344 (2011)
- Mahamud, M., López, O., Pis, J.J., Pajares, J.A.: Textural characterization of coals using fractal analysis. *Fuel Process. Technol.* **81**(2), 127–142 (2003)
- Mahamud, M.M., Novo, M.F.: The use of fractal analysis in the textural characterization of coals. *Fuel* **87**, 222–231 (2008)
- Mandelbrot, B.B.: *Les Objects Fractals: Forme, Hasard et Dimension*. Flammarion, Paris (1975)
- Mandelbrot, B.B.: *The Fractal Geometry of Nature*. W.H. Freeman, New York (1983)
- Ncibi, M.C., Jeanne-Rose, V., Mahjoub, B., Jean-Marius, C., Lambert, J., Ehrhardt, J.J., Bercion, Y., Seffen, M., Gaspard, S.: Preparation and characterisation of raw chars and physically activated carbons derived from marine *Posidonia oceanica* (L.) fibres. *J. Hazard. Mater.* **165**, 240–249 (2009)
- Przemyslaw, B.: On the relations between lacunarity and fractal dimension. *Acta Phys. Pol.* **40**(5), 1485–1490 (2009)
- Passé-Coutrin, N., Jeanne-Rose, V., Ouensanga, V.A.: Textural analysis for better correlation of the char yield of pyrolysed lignocellulosic materials. *Fuel* **84**, 2131–2134 (2005)
- Passé-Coutrin, N., Altenor, S., Cossement, D., Jean-Marius, C., Gaspard, S.: Comparison of parameters obtained from the BET and Freundlich isotherms obtained by nitrogen adsorption on activated carbons: a new method for calculating the specific surface area. *Microporous Mesoporous Mater.* **111**, 517–522 (2008)
- Tatlyer, M., Erdem-Suenatalar, A.: Method to evaluate the fractal dimensions of solid adsorbents. *J. Phys. Chem.* **103**, 4360–4365 (1999)